ISSN 1330–0016
CODEN FIZBE7

UNEXPECTED PROPERTY OF PROXIMITY POTENTIALS

RADU A. GHERGHESCU, WALTER GREINER* and DORIN N. POENARU*

Institute of Atomic Physics, P. O. Box MG-6, RO-76900 Bucharest, Romania
**Institut für Theoretische Physik der Universität, Robert-Mayer Strasse 8-10, Postfach 111932, D-60054 Frankfurt am Main 11, Deutschland*

Received 27 May 1994

UDC 539.17

PACS 25.85

The cold fission barriers of heavy and superheavy nuclei ($Z = 80 - 120$) are computed using two macroscopic models, the Yukawa-plus-exponential and the proximity potential. No shell and pairing corrections have been added. Unexpectedly, the barriers are showing two maxima in a wide region of nuclei ($Z = 96 - 120$, mostly neutron-deficient ones) and various mass and charge asymmetries, lower for lighter nuclei and larger for heavier ones. The rather shallow minimum separating the maxima can reach a depth of 37 keV in the Yukawa-plus-exponential model and 190 keV in the proximity potential model.

1. Introduction

The interest for study of the fission and fusion barriers is motivated by a possible existence (or synthesis by fusion reactions) [1] of superheavy nuclei, and by the production of metastable nuclear molecular states that allow testing the electrodynamics of strong field [2]. Most of the up to now performed calculations are related to the classical fission mechanism with elongated fragment shapes [3] rather than the cold fission processes [4] in which the fragments are not deformed.

The purpose of the present work is to present the calculations made using two frequently used macroscopic models, the Yukawa-plus-exponential model (Y+EM)[5] and the proximity potential model (PPM)[6], both taking into account the finite range of the nuclear forces. They have been developed as an alternative to the liquid drop model (LDM) which is known to have some drawbacks like, for example, the absence of any proximity attraction between separated nuclei at a small distance ($1 - 2$ fm) within the range of nuclear forces, and the neglect of surface diffusivity. It is generally accepted that the shape of the fission barrier (potential energy versus separation distance) shows a smooth behaviour: from a minimum at the ground state it increases up to a saddle point and then decreases smoothly again. To our surprise, the present calculations show a pocket in the potential barrier for a relatively low value of the separation tip distance of the fragments. Such a pocket is known to appear as a result of the microscopic shell and pairing effects, superposed on the macroscopic potential, causing the well known double-humped fission barrier introduced by Strutinsky.

The strong interaction between the two nuclear fragments continues to act even when they are separated within the range of the nuclear forces. As a result of a competition between the nuclear attraction and the Coulomb repulsion, the total fragment interaction energy can reach a maximum value for a certain combination of a parent nucleus and two fragments.

A nuclear shape parametrization of two intersected spheres has been used. It allows to describe continuously the shape transformation from one initial nucleus to two final nuclei, by changing the separation distance between the two centers and keeping the total volume constant. Each of the three reaction partners, the compound fissioning nucleus and the two fragments, have been selected by imposing the condition that they are listed in the table of atomic masses calculated by Möller et al. [7]. In this way we can select the nuclei of practical importance, up to the proton drip-line.

2. Yukawa-plus-exponential model extended to binary systems with different charge densities

The shape-dependent terms of the nuclear potential energy in a LDM are the surface energy due to strong interactions between all kind of nucleons, tending to hold them together, and the Coulomb interaction between protons, acting in the opposite direction. In order to take into account both the finite range of nuclear forces and the surface diffusivity, in the Y+EM model the nuclear energy, replacing the Myers-Swiatecki's liquid drop model surface energy, is given by the double folded Y+EM potential. During the cold fission process the nuclear shape is changed starting from a spherical compound nucleus, going through two intersected spheres with increasing separation distance between the centers and ending up with two well separated spherical fragments. The opposite direction is followed in a fusion reaction. The total volume of the system is conserved all the time.

The nuclear energy [5] is given by the following double volume integral:

$$E_Y = -\frac{c_s}{8\pi^2 r_0^2 a^4} \int_{V_n}\int \left(\frac{r_{12}}{a} - 2\right) \frac{\exp(-r_{12}/a)}{r_{12}/a} \mathrm{d}^3 r_1 \mathrm{d}^3 r_2, \tag{1}$$

where $r_{12} = \mid \vec{r}_1 - \vec{r}_2 \mid$, $a =$ 0.68 fm is the diffusivity parameter, $c_s = a_s(1 - \kappa I^2)$, $a_s =$ 21.13 MeV is the surface energy constant, $\kappa =$ 2.3 is the surface asymmetry constant and $r_0 =$ 1.16 fm is the nuclear radius constant.

We take into account the difference between the charge densities of the two fragments. This energy can be expressed [8] as a sum of two self-energies and an interaction energy between the fragments

$$E_Y = -\frac{c_{s1}}{8\pi^2 r_0^2 a^4} \int_{V_1} \mathrm{d}^3 r_1 \int_{V_1} \left(\frac{r_{12}}{a} - 2\right) \frac{\exp(-r_{12}/a)}{r_{12}/a} \mathrm{d}^3 r_2 -$$

$$-\frac{2\sqrt{c_{s1}c_{s2}}}{8\pi^2 r_0^2 a^4} \int_{V_1} \mathrm{d}^3 r_1 \int_{V_2} \left(\frac{r_{12}}{a} - 2\right) \frac{\exp(-r_{12}/a)}{r_{12}/a} \mathrm{d}^3 r_2 -$$

$$-\frac{c_{s2}}{8\pi^2 r_0^2 a^4} \int_{V_2} \mathrm{d}^3 r_1 \int_{V_2} \left(\frac{r_{12}}{a} - 2\right) \frac{\exp(-r_{12}/a)}{r_{12}/a} \mathrm{d}^3 r_2 . \tag{2}$$

The relative nuclear energy B_Y is normalized to the spherical shape one, E_Y^0:

$$B_Y = \frac{E_Y}{E_Y^0} = \frac{c_{s1}}{c_{s0}} B_{Y1} + \frac{\sqrt{c_{s1}c_{s2}}}{c_{s0}} B_{Y12} + \frac{c_{s2}}{c_{s0}} B_{Y2}, \tag{3}$$

where B_{Y1}, B_{Y2} correspond to the two fragments and B_{Y12} is the interaction term. For overlapping fragments with axial symmetry, the involved three-dimensional integrals are calculated numerically by the Gauss-Legendre quadrature.

For a spherical compound nucleus with a radius $R_0 = r_0 A^{1/3}$ one obtains:

$$E_Y^0 = c_{s0} A^{2/3} \{1 - 3x^2 + (1 + 1/x)[2 + 3x(1 + x)]e^{-2/x}\}, \tag{4}$$

where $x = a/R_0$.

The Coulomb energy is calculated in a similar way:

$$E_C = \frac{\rho_{1e}^2}{2} \int_{V_1} \mathrm{d}^3 r_1 \int_{V_1} \frac{\mathrm{d}^3 r_2}{r_{12}} + \rho_{1e}\rho_{2e} \int_{V_1} \mathrm{d}^3 r_1 \int_{V_2} \frac{\mathrm{d}^3 r_2}{r_{12}} + \frac{\rho_{2e}^2}{2} \int_{V_2} \mathrm{d}^3 r_1 \int_{V_2} \frac{\mathrm{d}^3 r_2}{r_{12}}, \tag{5}$$

where the first two terms are due to the individual fragments and the third one represents their interaction. The charge densities of the compound nucleus and of the two fragments are denoted by ρ_{0e}, ρ_{1e} and ρ_{2e}, respectively.

The relative Coulomb energy is given by:

$$B_C = \frac{E_C}{E_C^0} = \left(\frac{\rho_{1e}}{\rho_{0e}}\right)^2 B_{C1} + \frac{\rho_{1e}\rho_{2e}}{\rho_{0e}} B_{C12} + \left(\frac{\rho_{2e}}{\rho_{0e}}\right)^2 B_{C2}, \tag{6}$$

where B_{C1} and B_{C2} are the Coulomb relative energies of the fragments, B_{C12} is the relative Coulomb interaction term (two dimensional integrals for axially symmetric overlapping fragments), and

$$E_C^0 = \frac{3e^2 Z^2}{5 r_0 A^{1/3}} \tag{7}$$

is the Coulomb energy for a spherical nucleus with a mass number A.

The total deformation energy is the sum of Y+E, Coulomb and of the volume terms:

$$E = E_Y + E_C + E_V. \tag{8}$$

When the fragments are separated ($R > R_t = R_1 + R_2$), analytical relationship are available:

$$E_C = \frac{Z_1 Z_2 e^2}{R} \tag{9}$$

$$E_Y = -4\left(\frac{a}{r_0}\right)\sqrt{c_{s1}c_{s2}}\left[g_1 g_2 (4 + \frac{R}{a}) - g_2 f_1 - g_1 f_2\right]\frac{e^{-R/a}}{R/a}, \tag{10}$$

where:

$$f_k = \left(\frac{R_k}{a}\right)^2 \sinh\frac{R_k}{a}, \tag{11}$$

$$g_k = \frac{R_k}{a}\cosh\frac{R_k}{a} - \sinh\frac{R_k}{a}, \quad (k = 1, 2) \tag{12}$$

and R is the distance between the centers of the two fragments.

3. Proximity potential

In the macroscopic model the proximity potential introduced by Blocki and Swiatecki [6], for two separated fragments, is given by:

$$E_{pr} = \int\int e(D)\mathrm{d}x\mathrm{d}y, \tag{13}$$

where $e(D)$ is the interaction energy per unit area between plane, parallel surfaces at a separation D, and the integration is performed in the transverse $x0y$ plane perpendicular to the line of least separation.

The universal dimensionless proximity function $\varphi(\zeta)$ is introduced. It gives the energy density e in units of 2γ, where γ is the specific surface energy of the order of 1 MeV/fm^2. One can express the least separation distance s between surfaces in units of the surface width b of the order of 1 fm, $s = \zeta b$. Then:

$$e(\zeta b) = 2\gamma\Phi(\zeta), \tag{14}$$

where Φ is the interaction energy per unit area in units of 2γ. Due to the short range of nuclear forces, Φ vanishes at large separation.

For practical calculations one has:

$$E_{pr} = 4\pi\gamma\overline{R}\Phi(\zeta), \tag{15}$$

where the mean curvature radius $\overline{R}$ is given by:

$$\overline{R} = \frac{C_1 C_2}{C_1 + C_2} \tag{16}$$

in which $C_i = R_i - b^2/R_i$, $(i = 1, 2)$ are the central radii and $R_i = 1.28A^{1/3} - 0.76 + 0.8A^{-1/3}$ are the effective sharp radii; the subscript i refers to the two fragments or to the compound nucleus.

The nuclear proximity function has been calculated in the Thomas-Fermi approximation with effective two-nucleon Seyler-Blanchard interaction. A good approximation to the integrated function Φ was found [6] to be:

$$\Phi(\zeta) = \begin{cases} -1.7817 + 0.927\zeta + 0.01696\zeta^2 - 0.05148\zeta^3 & 0 \leq \zeta \leq 1.9475 \\ -4.41\exp(-\zeta/0.7176) & \zeta > 1.9475 \end{cases} \tag{17}$$

and for overlapping spheres:

$$\Phi(\zeta) = -1.7817 + 0.927\,\zeta + 0.143\,\zeta^2 - 0.09\,\zeta^3 \quad \zeta \geq 0. \tag{18}$$

The surface coefficient γ is taken as:

$$\gamma = 0.9517[1 - 1.7826(1 - 2Z/A)^2]\ \text{MeV/fm}^2. \tag{19}$$

The Coulomb interaction energy expression is identical to the one calculated in Section 2.

4. *Results*

Previously, we have performed similar calculation within the Y+EM at symmetry [9]. In this work, we consider both Y+EM and PPM and the entire range of mass and charge asymmetries. With each of the two macroscopic models, we have obtained a rather wide region in the $(Z,\, N)$ nuclear chart, in the heavy and superheavy range of nuclei, characterized by the two-humped cold fission barrier shapes. This result is a consequence of the use of the proximity potentials and will be discussed in the next Section.

The first maximum of the potential barrier lays within a few tenths of fm beyond the touching point $R_M^{(1)} \geq R_t$. The second maximum appears always at a larger separation distance between the fragments, $R_M^{(2)} > R_M^{(1)}$.

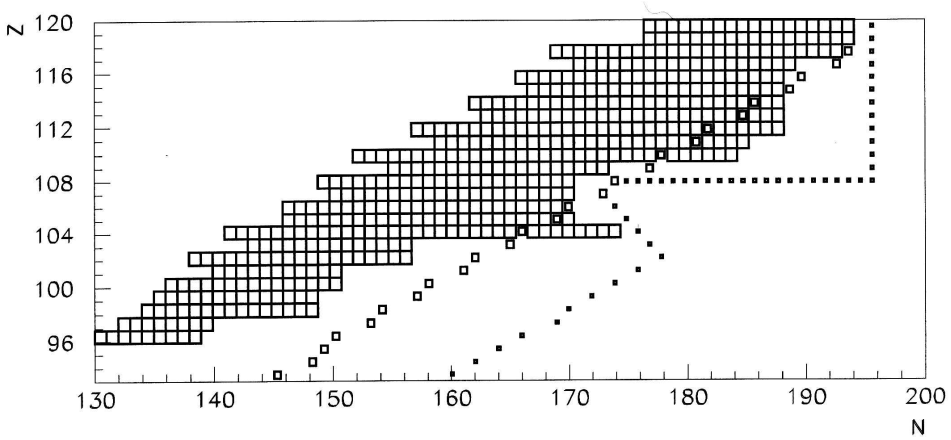

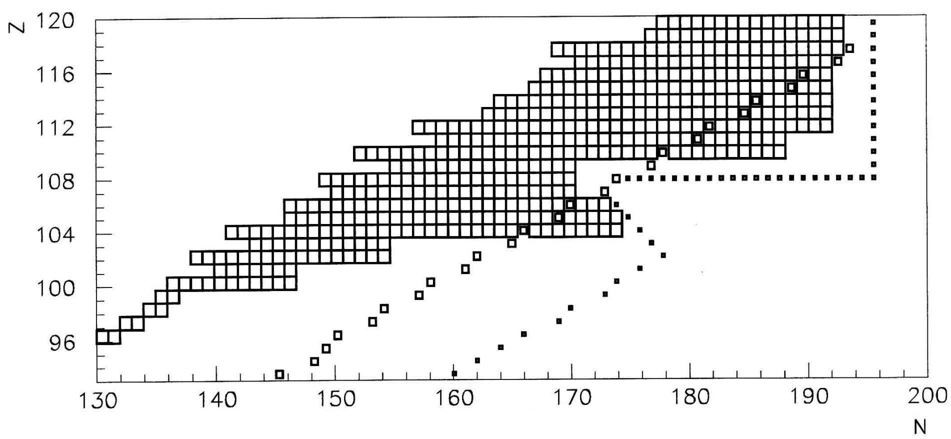

Fig. 1. The larger boxes represent nuclei showing two-humped cold fission barriers in the Y+EM *(upper) and* PPM *(lower diagram). The smaller boxes show the line of beta-stability derived from the Green approximation. The small squares show the border of neutron-rich nuclei according to (7).*

The boxes in the nuclear chart in Fig. 1 (upper plot for Y+EM and lower plot for PPM) represent the compound nuclei showing a barrier shape with two maxima for at least one pair of values of the charge and mass asymmetry parameters, $\eta_Z = (Z_H - Z_L)/Z$ and $\eta_A = (A_H - A_L)/A$.

By definition, the depth of the minimum, Δe, situated at $R = R_M$ between the two maxima (each of them at $R_M^{(1)}$ and $R_M^{(2)}$, respectively), where $R_M^{(1)} < R_M < R_M^{(2)}$, is given by:

$$\Delta e = \min[E(R_M^{(1)}), E(R_M^{(2)})] - E(R_M). \qquad (20)$$

In Table 1 we have selected the largest depths of the pockets for each even value of Z for the Y+EM (left) and for the PPM (right) for all heavy even-even nuclei exhibiting the two-humped barrier shapes.

TABLE 1.

The largest depths of the pockets in the cold fission potential barrier of some even-even nuclei for Y+EM *and* PPM.

	Y+EM						PPM					
Z	A	Z_L	Z_H	A_L	A_H	Δe/keV	A	Z_L	Z_H	A_L	A_H	Δe/keV
96	230	46	50	96	134	24	232	10	86	20	212	1
98	232	46	52	96	136	26	232	46	52	96	136	4
100	242	46	54	100	142	20	238	46	54	96	142	38
102	244	46	56	104	142	30	240	46	54	96	144	166
104	258	46	58	108	150	32	246	50	54	116	130	190
106	256	30	76	60	196	37	256	50	56	128	128	186
108	262	38	70	96	166	29	266	42	66	96	170	180
110	274	34	76	76	198	31	266	34	76	72	194	183
112	272	30	82	64	208	34	272	30	82	60	112	180
114	278	26	88	52	226	33	282	30	84	68	214	176
116	284	30	86	68	216	29	292	38	78	92	200	164
118	304	30	88	68	240	28	296	38	80	100	196	171
120	302	30	90	72	230	27	298	34	86	84	214	164

Assuming the same conditions, the complete results of calculations in the PPM are shown in Fig. 2. In the Figs. 2a,b, the maximum values of Δe for pairs of values (η_Z, Z) are presented. The three-dimensional plots in Fig. 2c,d show the corresponding mass numbers A and A_L of the compound nucleus and the light fragment, respectively.

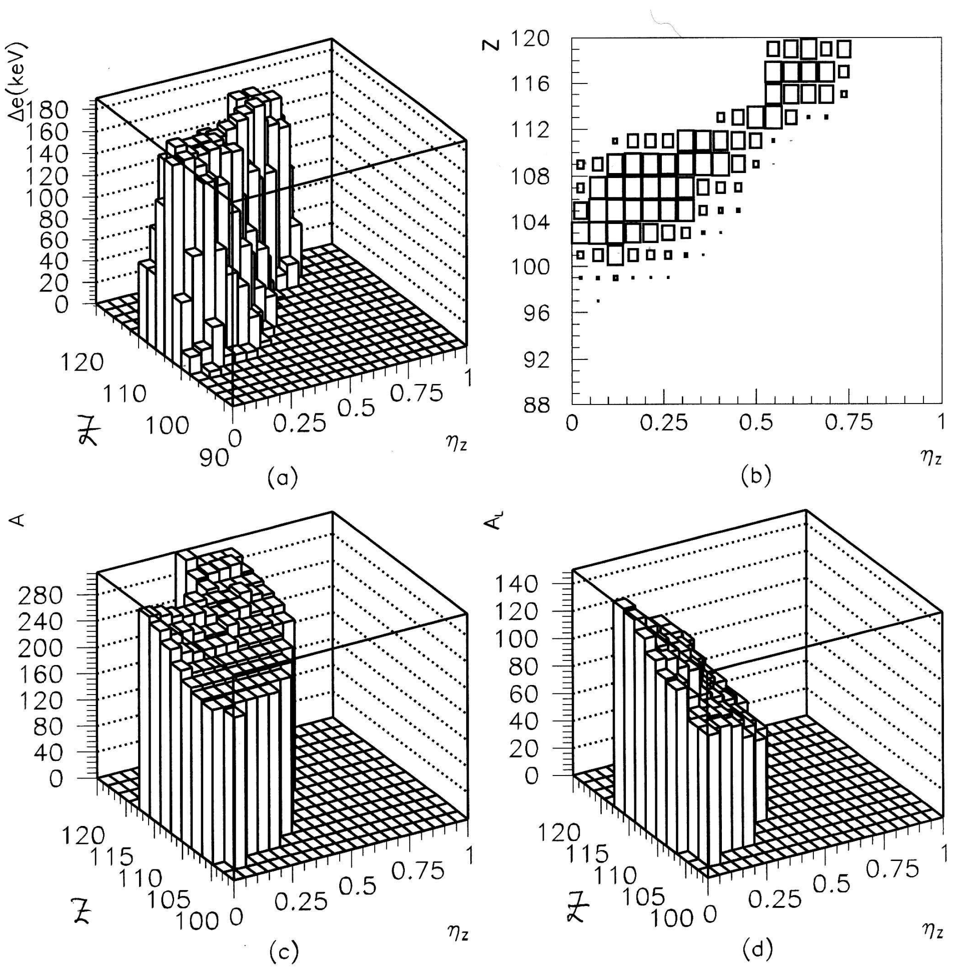

Fig. 2. Results obtained in the PPM *for the largest values of the pocket depths Δe: (a) versus the charge asymmetry parameter η_Z and the atomic number Z of the compound nucleus;*
(b) the same relationship represented by boxes of a size proportional to Δe.
In the following two plots the corresponding mass numbers of the compound nucleus (c) and of the light fragment (d) can be seen.

The trend toward a larger value of the charge asymmetry parameter η_Z, at which Δe is maximum, with increasing atomic number Z of the compound nucleus is clearly seen in Fig. 2b.

Almost the same values of the parameters η_Z appear in similar plots illustrating the results obtained in the Y+EM. The richest elements in combinations parent

(A, Z)-fragments (A_L, Z_L), (A_H, Z_H) leading to maximum values of Δe are $Z = 104$ and $Z = 106$, both for the Y+EM and PPM. In the Y+EM the deepest pocket in the barrier shape is obtained for $Z = 106$; it is 37 keV for $Z_L/Z_H = 30/76$ and $A_L/A_H = 60/196$. Within the PPM the maximum is much larger: 190 keV for $Z = 106$ with $Z_L/Z_H = 50/56$ and $A_L/A_H = 128/128$.

The similarity of the results obtained in both models can also be seen in Fig. 3, where the three-dimensional plots of Δe against the mass asymmetry η_A and the mass number of A refer to $Z = 104$ and $Z_L = 46$.

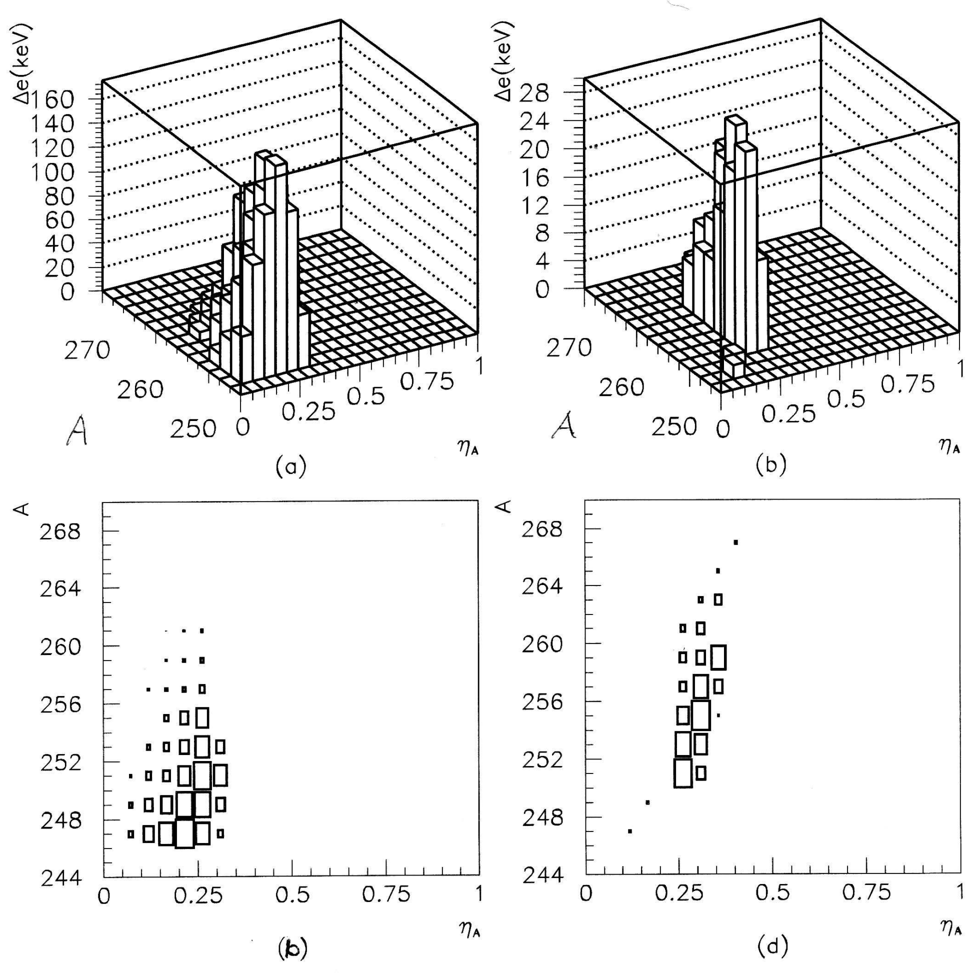

Fig. 3. The pocket depths versus the mass asymmetry η_A and the mass number A of the compound nucleus for the isotopes of $Z = 104$, and the light fragment $Z_L = 46$ (a, b) in the PPM *and (c, d) in the* Y+EM.

5. *Discussion*

The evolution of the two-humped barrier in the PPM with the mass number A and the mass asymmetry η_A is ploted in Fig. 4, for $Z = 104$. The fragment mass numbers $A_L - A_H$ are specified. One should mention that in the Y+EM approach, a similar behaviour is observed.

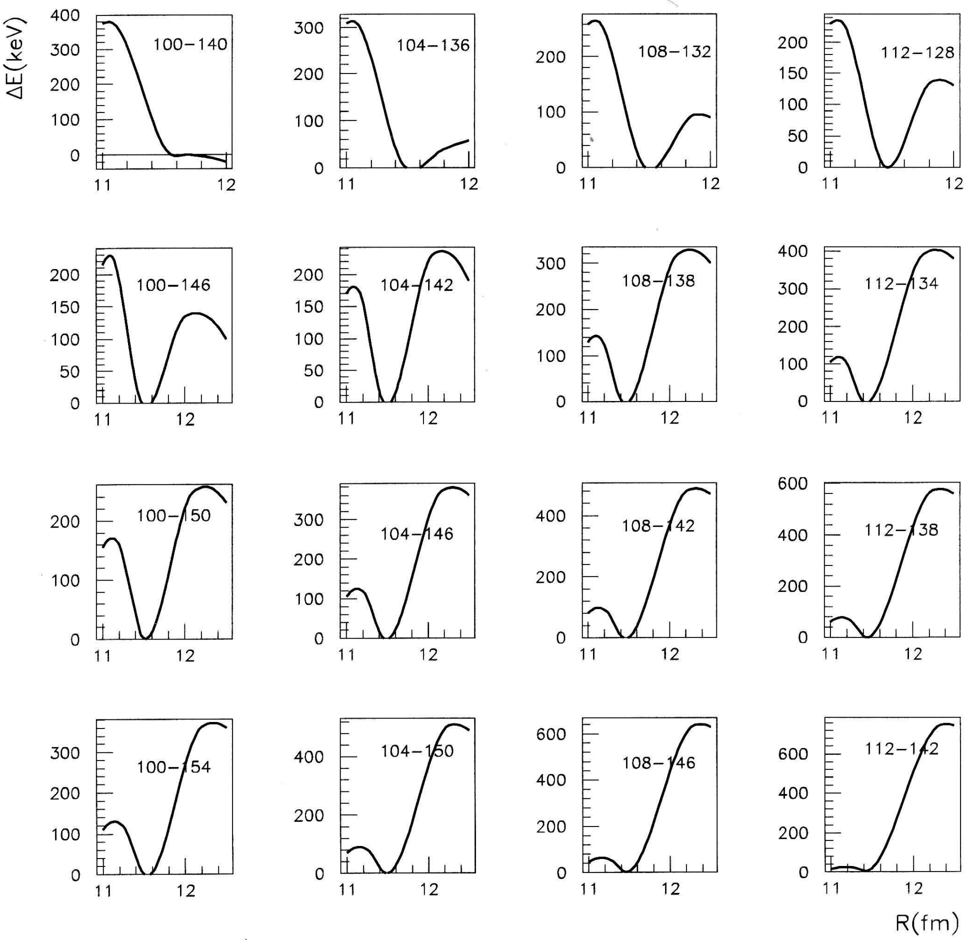

Fig. 4. Details of the PPM *barrier shapes in a small region of separation distance beyond the touching point configuration, for $Z = 104$ and $Z_L = 46$. The two numbers shown on each plot are the mass numbers of the fragments, A_L and A_H.*

Only a small region of $\Delta e = E - E(R_m)$, including the two maxima beyond the touching point configuration ($R \geq R_t$) is plotted. The transition from one maximum at the touching point (or very close to the touching point) toward two maxima, can be clearly seen. When the mass number of the light fragment A_L increases from 100 to 112 and the mass number of the compound nucleus, $A = A_L + A_H$, is raised from 240 to 245, we obtain various two-humped barrier shapes with the first barrier height larger, equal or smaller than the second one. For a given A, the depth of the pocket reaches its maximum value when the two heights are approximately equal. Then, the first maximum decreases with the increase of the second one and finally the pocket disappears. At the same time the second maximum moves away from the touching-point configuration. The second energy hump reaches its maximum value when the first one has almost totally disappeared.

In the following, we shall analyze the conditions that yield the two-humped barrier shape. In the Y+EM, for separated fragments, neglecting the volume term, the interaction energy (8) can be written as:

$$E(r) = \frac{c_1}{r} + c_2 \frac{e^{-r}}{r} + c_3 e^{-r}, \tag{21}$$

where: $r = R/a$, $R = R_t + D$, D is the separation distance of the fragment surfaces, and

$$c_1 = Z_1 Z_2 e^2 / a$$

$$c_2 = -4(a/r_0)^2 \sqrt{c_{s1} c_{s2}} (4 g_1 g_2 - f_2 g_1 - f_1 g_2)$$

$$c_3 = -4(a/r_0)^2 \sqrt{c_{s1} c_{s2}} g_1 g_2 .$$

In order to study the critical points of the function $E(r)$, one has to calculate its derivate with respect to r:

$$\frac{\mathrm{d}E(r)}{\mathrm{d}r} = -\frac{c_1}{r^2} - c_2 \frac{e^{-r}(r+1)}{r^2} - c_3 e^{-r} \tag{22}$$

in the interval of interest (r_1, r_2), where $r_1 = r_t = R_t/a$, and $r_2 \approx r_t + 1.5$, taking into account that the position of the second maximum $R_M^{(2)} \leq R_t + 1.0$ fm. The two functions, $E(r)$ and $\mathrm{d}E(r)/\mathrm{d}r$ are plotted in Fig. 5, for $Z = 102$, $Z_L = 38$, $A = 244$ and five different values of the mass asymmetry parameter in the range $A_L = 76 - 78$.

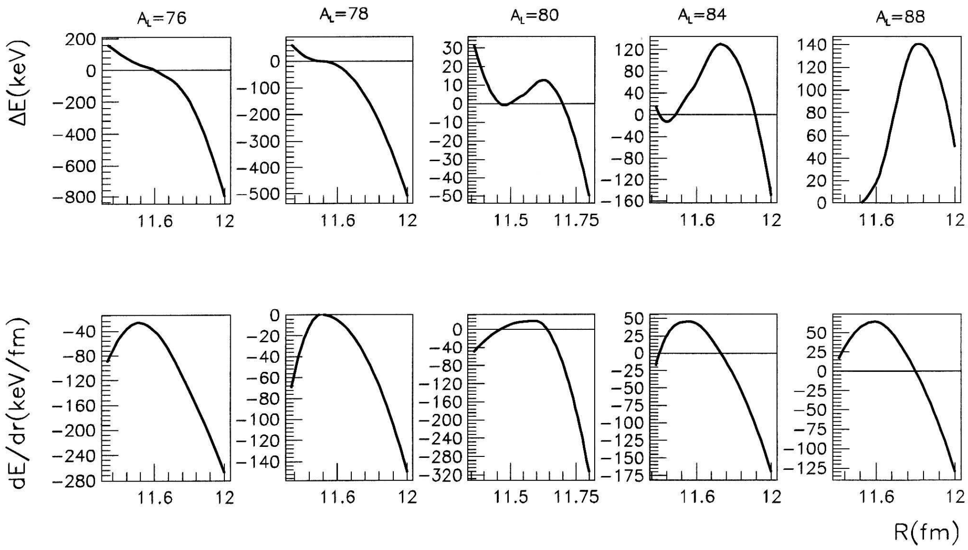

Fig. 5. Heights Δe *of the energy maxima above the minimum value and its derivative* $\mathrm{d}E/\mathrm{d}r$ *in the* Y+EM *vs. separation distance between the fragment centers, for* $Z = 102$, $A = 244$, $Z_L = 38$.

The derivative with respect to R has the dimension of a force, hence, up to a multiplicative constant, one can say that $\mathrm{d}E/\mathrm{d}r$ is proportional to the sum of the repulsive Coulomb force and the attractive strong interaction. The evolution of $\mathrm{d}E/\mathrm{d}r$ is the result of the equilibrium between the two forces or the domination of one of them over the other.

One can see (Fig. 5) that, in the case of a single maximum of the barrier at the touching point, the Coulomb force dominates, hence the sign of the resultant is negative. As A_L increases, the maximum of the derivative reaches the Or axis, corresponding to an inflection point of the barrier shape function ($\mathrm{d}^2E/\mathrm{d}r^2 = 0$). For larger values of A_L, there are two intercepts of the derivative with the Or axis. The first root represents a minimum (the pocket) and the second one is the second maximum. By adding more neutrons to the light fragment, the difference between the two forces increases in favour of the attractive one, leading to the disappearance of the pocket. Finally there is only the second maximum left.

When the two maxima are comparable, they are very close to each other. As the second one increases, it moves away from the touching point.

Let us introduce a new variable, x, representing the separation distance between the fragments tips, defined by:

$$r = r_t + x. \tag{23}$$

In the region of two maxima, $r \in (r_1, r_2)$, x is usually a small quantity, $x \ll 1$. Hence to a good approximation, we can retain only few terms in the expansion of $\mathrm{d}E/\mathrm{d}r$ around $x = 0$,

$$\frac{\mathrm{d}E}{\mathrm{d}r} \approx ax^3 + bx^2 + cx + d. \tag{24}$$

It will have positive roots if the following conditions are fulfilled:

$$\begin{gathered} b^2 - 3ac > 0 \\ \frac{b^2(4bd - c^2)}{27a^2} + d^2 + \frac{4c^3}{27a} - \frac{2bcd}{3a} < 0 \\ a < 0, \quad b > 0, \quad c < 0, \quad d > 0 \end{gathered} \tag{25}$$

where:

$$a = c_1 e^{r_t}/6$$

$$b = c_1 e^{r_t}/2 + c_3$$

$$c = c_1 e^{r_t} + c_2 + 2c_3 r_t$$

$$d = c_1 e^{r_t} + c_2 + 2c_3 r_t.$$

The potential barrier will have two maxima if the conditions (25) are satisfied.

In the PPM we get a forth order polynomial for the expansion $\mathrm{d}E/\mathrm{d}r$ around $x = 0$. In a similar way one can obtain the relationship between the coefficients that allow three real positive roots.

In conclusion, by studying the macroscopic cold fission or fusion barrier shapes of heavy and superheavy nuclei with $Z = 80 - 120$ in a wide range of mass and charge asymmetry in the Y+EM and PPM, we have found a whole region of mostly neutron-deficient nuclei that show two-humped barriers for separated spherical fragments. The minimum and the second maximum are relatively close to the touching point configuration, within the range of the strong interaction. The result is due to the used nuclear potentials; it would not show up in the Myers-Swiatecki's liquid drop model. The pocket between the two maxima is rather shallow: 37 keV in the Y+EM and not larger than 190 keV in the PPM. This behaviour of a phenomenological potential, that is expected to be smooth, seems to be unphysical. The result is a consequence of the particular expression for the nuclear energy term (replacing the surface energy in the liquid drop model) that was added to the Coulomb interaction, which is always monotonously decreasing with increasing separation distance between the fragments.

Acknowledgments

This work is supported by the Bundesministerium für Forschung und Technologie, the Deutsche Forschungsgemeinschaft, and the Institute of Atomic Physics. One of us (D.N.P.) has received a donation of computer equipment from the Soros Foundation for an Open Society.

References

1) U. Mosel and W. Greiner, Z. Phys. **222** (1969) 261;
A. Sobicsewski, in *Nuclei Far From Stability/Atomic Masses and Fundamental Constants* 1992, Inst. Phys. Conf. Ser. No 132, edited by R. Neugart and A. Wöhr (IOP Publishing Ltd, Bristol, 1993), p. 403;

2) W. Greiner, B. Müller and J. Rafelski, *Quantum Electrodynamics of Strong Fields* (Springer, Berlin, 1985);

3) P. Armbruster, Journal Physical Society Japan, Suppl. **58** (1989);

4) F. Gönnenwein in: *The Nuclear Fission Process*, edited by C. Wagemans (CRC Press, Boca Raton, Florida, 1991), p. 387;
E. K. Hulet, in proc. 5th *International Conference on Nuclei far from Stability*, Rosseau Lake, Canada, AIP Conference Proceedings No. 164, edited by I. S. Towner, (American Institute of Physics, New York, 1988), p. 810;

5) W. Scheid and W. Greiner, Z. Phys. **226** (1969) 364;
H. J. Krappe, J. R. Nix and A. J. Sierk, Phys. Rev. C **20** (1979) 992;

6) J. Blocki, J. Randrup, W. J. Swiatecki and K. F. Tsang, Ann. Phys. (N. Y.) **105** (1977) 427;

7) P. Möller, J. R. Nix, W. D. Myers and W. J. Swiatecki, Atomic Data Nucl. Data Tables **39** (1992);

8) D. N. Poenaru, M. Ivascu and D. Mazilu, Comp. Phys. Comm. **19** (1980) 205;

9) R. Gherghescu and D. N. Poenaru, Rom. J. Phys. **37** (1992) 1005.

NEOČEKIVANA SVOJSTVA BLIZINSKOG POTENCIJALA

RADU A. GHERGHESCU, WALTER GREINER* i DORIN N. POENARU*

Institute of Atomic Physics, P. O. Box MG-6, RO-76900 Bucharest, Romania
**Institut für Theoretische Physik der Universität, Robert-Mayer Strasse 8-10, Postfach 111932, D-60054 Frankfurt am Main 11, Deutschland*

UDK 539.17

PACS 25.85

Fisijski bedemi teških i superteških jezgri ($Z = 80 - 120$) određeni su u dva makroskopska modela (Yukawa + eksponencijalni potencijal i blizinski potencijal) ne izračunavajući korekcije ljuske i sparivanje. U širokom području jezgri ($Z = 96 - 120$, uglavnom s manjkom neutrona), različitih masa i asimetrija naboja, bedemi imaju dva maksimuma, koji su niži za lakše jezgre a viši za teže jezgre. Plitki minimum između maksimuma doseže dubinu 37 keV u Yukawa + eksponencijalnom modelu i 190 keV u modelu blizinskog potencijala.